Two-dimensional simulations of extreme floods on a large watershed

John F. England Jr. [a,*], Mark L. Velleux [b], Pierre Y. Julien [c]

[a] *Bureau of Reclamation, Flood Hydrology, 86-68530, Denver Federal Center, Denver, CO 80225, USA*
[b] *HydroQual, Inc., Mahwah, NJ 07430, USA*
[c] *Department of Civil Engineering, Colorado State University, Fort Collins, CO 80523, USA*

Summary   We investigate the applicability of the Two-dimensional, Runoff, Erosion and Export (TREX) model to simulate extreme floods on large watersheds in semi-arid regions in the western United States. Spatially-distributed extreme storm and channel components are implemented so that the TREX model can be applied to this problem. TREX is demonstrated via calibration, validation and simulation of extreme storms and floods on the 12,000 km^2 Arkansas River watershed above Pueblo, Colorado. The model accurately simulates peak, volume and time to peak for the record June 1921 extreme flood calibration and a May 1894 flood validation. A Probable Maximum Precipitation design storm is used to apply the calibrated model. The distributed model TREX captures the effects of spatial and temporal variability of extreme storms for dam safety purposes on large watersheds, and is an alternative to unit-hydrograph rainfall-runoff models.
© 2007 Elsevier B.V. All rights reserved.

Introduction

The estimation and prediction of extreme floods is a central theme in hydrologic engineering and dam safety (Swain et al., 2004). Mathematical watershed models are used to describe or simulate extreme floods. These models usually have two purposes in hydrology: the first is to explore the implications of making certain assumptions about the nature of the real world system; the second is to predict the behavior of the real world system under a set of naturally-occurring circumstances (Beven, 1989). One main reason to use a rainfall-runoff model is because we have not measured the variable of interest and need a way to extrapolate those measurements (Beven, 2001).

The watershed models that are extensively used to simulate extreme floods and Probable Maximum Floods (PMFs) are, in most cases, unit hydrograph or storage routing models. In the United States, the HEC-1 (HEC, 1998) and HEC-HMS models (HEC, 2006) are used by the Corps of Engineers, and the Flood Hydrograph and Runoff (FHAR) model (Reclamation, 1990) is used by the Bureau of Reclamation. These models based on unit hydrographs are used nearly

---

exclusively for dam safety. On occasion other models, such as variants to the Stanford Watershed model, have been used for PMF estimation (Cecilio et al., 1974). In the United Kingdom, the national flood guidelines specify the use of a unit hydrograph model for extreme flood runoff and PMF calculations (IH, 1999). Similarly, the Australian Rainfall-Runoff guidelines for extreme flood estimation, published in 1987, have been revised (ARR, 2001). They recommend using unit hydrograph or storage routing models such as RORB (Laurenson et al., 2006). Nathan and Weinmann (1999) provide guidance on choosing between unit hydrograph or storage models in Australia. Pilgrim and Cordery (1993) summarize these unit hydrographs and flood hydrograph models in current practice.

To capitalize on recent research developments, we explore the use of a physically-based and distributed model to estimate extreme floods on large watersheds. Following Singh (1995), we define a large watershed as one with a drainage area that exceeds 1000 km². Ponce (1989) suggested one should use routing-based methods rather than unit hydrographs for large watershed flood runoff. Dunne (1998) noted that on drainage areas exceeding 10^4 km², statistical analysis of floods is favored over physical theory; he suggested a focus is needed on processes that actually generate floods, including extreme runoff generation and large rainstorms. Important flood processes on large watersheds can include: infiltration (Smith, 2002); overland flow routing (Troch et al., 1994); channel storage and processes (Singh, 1995); partial area storms (Marco and Valdés, 1998), runoff and runon (Woolhiser, 1996); and antecedent conditions (Woolhiser et al., 1996). Over 100 years ago, Murphy and others (1906) recognized that size of the drainage basin and physiography were important flood physical processes. Garbrecht and Shen (1988) showed that the rainfall, overland flow, channel flow and channel network phases affect runoff, peak and timing, and that peak flow in a channel is a function of the overland and channel flow processes and the drainage network. Spatially varying parameters in the drainage network and channel geometry affect the peak flow, time to peak, and hydrograph duration (Saco and Kumar, 2002a), the parameters change across scales (Saco and Kumar, 2002b), and are one explanation for the observed nonlinear response in watersheds (Paik and Kumar, 2004). The representation of hillslopes and channels clearly affects travel times and hydrologic response (D'Odorico and Rignon, 2003). Saco and Kumar (2004) suggest that even on large basins it is crucial to simulate hillslope dynamics. The model used in our work incorporates these important spatially-varying physical processes.

The focus of this research is to improve and test a physically-based rainfall-runoff model in order to simulate extreme floods on large watersheds for dam safety considerations. The goal is to have a practical and tested alternative to the current lumped-parameter unit hydrograph watershed models used to simulate extreme floods in the western United States. The Two-dimensional, Runoff, Erosion and Export (TREX) model (Velleux et al., 2006a,b) is central to the effort. The specific objectives are to: (1) describe new model features for extreme storms and channel networks on large watersheds; and (2) demonstrate the applicability of the TREX model through calibration, validation and simulation of extreme floods. The model is tested on a large (12,000 km²) watershed, the Arkansas River at Pueblo, Colorado. The physically-based model incorporates spatially-varied storm, hillslope and channel processes relevant to addressing solutions to extreme flood problems for dam safety (Cudworth, 1989; Swain et al., 2004).

TREX model

The physically-based TREX model is fully distributed and simulates rainfall-runoff, sediment transport, and chemical fate and transport at the watershed scale (Velleux et al., 2006a,b). TREX is based on the CASC2D model (Julien and Saghafian, 1991; Julien et al., 1995; Ogden and Julien, 2002; Julien and Rojas, 2002), and the WASP/IPX model (Ambrose et al., 1993; Velleux et al., 2001). The hydrology, sediment transport and chemical transport processes and components of TREX are described in Velleux et al. (2006a). The major hydrology components of the model include: rainfall, interception, surface storage, infiltration, and overland and channel runoff routing. The Green and Ampt equation is used to represent infiltration. Overland flow is estimated in two dimensions via the continuity equation and the momentum equation using the diffusive wave approximation. Channel flow is estimated in one dimension using the diffusive wave approximation. TREX is classified as an event model as it simulates the Hortonian (overland flow) surface watershed response from a single storm with no soil infiltration capacity recovery between events.

The most recent developments and applications with CASC2D and TREX have been in upland and watershed erosion and sediment transport (Molnar and Julien, 1998; Johnson et al., 2000; Rojas-Sanchez, 2002; Julien and Rojas, 2002), and chemical transport (Velleux et al., 2006b). TREX and CASC2D have not yet been applied on watersheds exceeding about 2000 km², or for estimating very extreme floods approaching the PMF (Table 1). Improvements to TREX are made in two main areas: storm rainfall modeling; and channel network pre-processing and parameterization. The new enhancements expand the capabilities of the model to simulate extreme floods up to the PMF on large watersheds.

Extreme storms

In order to successfully model extreme storms on large watersheds, additional rainfall techniques are added to TREX as part of this research. These include replacing the temporal interpolation method, modifying the rain gage spatial interpolation algorithm, re-implementing use of radar data, and including design storm and space—time depth—area duration (DAD) storm techniques.

The rainfall input to TREX consists of a time series of rainfall intensity and time ''pairs'' for each rain gage that is specified. The original temporal interpolation scheme was to use a constant value equal to the previous rainfall intensity observation for each gage between time steps. This concept has been replaced with a piecewise linear interpolation scheme between observation pairs i and $i + 1$. For each rain gage g ($g = 1$, nrg) the rainfall intensity r [L/T] at time increment t_j (function of model time step Δt) is:

Table 1 CASC2D and TREX applications and watershed sites

River/watershed	Drainage area (km^2)	Main purpose	References
Goodwin Creek, MS	20.7	Hydrology and Sediment Transport Calibration/ Prediction	Johnson et al. (2000), Senarath et al. (2000) and Julien and Rojas (2002)
Hickahala/Senatobia, MS	560	Hydrology and Grid Cell Size	Molnar and Julien (2000)
Taylor Arroyo, CO	120	Effects of Military Maneuvers	Ogden and Julien (1993) and Doe et al. (1996)
Spring Creek, CO	25	Flash Flood Modeling	Ogden et al. (2000)
Hassayampa Creek, AZ	1111	Flash Flood Forecasting	Jorgeson (1999)
Cave Creek, AZ	349	Flash Flood Forecasting	Jorgeson (1999)
Macks Creek, ID	32	Hydrology/Model Demonstration and Testing	Julien and Saghafian (1991) and Saghafian (1992)
Little Washita, OK	535.5	Initial Soil Moisture, Infiltration	Spah (2000)
Quebrada Estero, Costa Rica	2.5	Land cover change	Marsik and Waylen (2006)
California Gulch, CO	30	Metals transport	Velleux et al. (2006b)

$$r_g(t_j) = b_g(t) + m_g(t)\left(t_i + \sum_{j=1}^{n} \Delta t\right) \quad \text{for } \left(t_i + \sum_{j=1}^{n} \Delta t\right) \leqslant t_{i+1}$$

$$(1)$$

where $b_g(t)$ is the intercept estimated by

$$b_g(t) = r_g(t)_{i+1} \tag{2}$$

and $m_g(t)$ is the slope estimated by

$$m_g(t) = \frac{r_g(t)_{i+1} - r_g(t)_i}{t_{i+1} - t_i} \tag{3}$$

and n is an integer number of time steps between t_i and t_{i+1} with any remainder time added as a last step. This temporal interpolation scheme is used for all the new rainfall options. Four spatial rainfall options are now operational in the model: inverse-distance weighting (IDW) with rain gages; constant in space over user-specified areas for design storms; restricted nearest neighbor with radar data; and elliptical storms with depth-area duration (DAD) data.

The existing inverse-distance squared spatial interpolation algorithm is modified to a more flexible inverse-distance weighting (IDW) approach. Two changes are made: introducing a user-defined exponent (or power) parameter instead of a strict value equal to 2, and adding a radius of influence parameter. The general spatial interpolation problem described here is based on Tabios and Salas (1985) and Salas et al. (2002). We define rainfall gage coordinates in a regular square grid as x_j and y_j. The rainfall process at this gage j is defined as h_j, where the number of rain gages (nrg) is defined by $j = 1, 2, \ldots, nrg$. An estimate of the rainfall process (rate or depth) is defined as h_o at any point in space (x_o, y_o). This process h_o can be estimated by a weighted linear combination of the observations via:

$$h_o = \sum_{j=1}^{nrg} w_j h_j \tag{4}$$

where w_j is the weight of rainfall gage j. This weight is a function of the distance d_{oj} between h_o and h_j. TREX uses a straight-line distance estimator:

$$d_{oj} = \sqrt{(x_o - x_j)^2 + (y_o - y_j)^2} \quad j = 1, \ldots, nrg. \tag{5}$$

The weight w_j for station h_j is (Tabios and Salas, 1985):

$$w_j = \frac{f(d_{oj})}{\sum_{j=1}^{nrg} f(d_{oj})}, \tag{6}$$

where $f(d_{oj})$ represents a function of the distance d_{oj} between the estimation point h_o and the gage h_j. The new power function that is implemented is:

$$f(d_{oj}) = \begin{cases} \dfrac{1}{d_{oj}^{\alpha}} & d_{oj} \leqslant d_{max}, \\ 0 & \text{otherwise}. \end{cases} \tag{7}$$

Common values for α are 1, 1.5 and 2. Simanton and Osborn (1980) tested α values from 0 to 4.0 for summer thunderstorm rainfall and recommended using 1.0 in areas where air-mass thunderstorms dominate. If α is 1, the function is known as reciprocal distance, and if α is 2 it is called the inverse distance squared method. If higher values of this exponent are used, less weight is given to gages at increasing distance from the estimate point h_o. A restriction is placed on d_{oj}, with a radius of influence parameter d_{max} defined to be the maximum distance between the point of interest (x_o, y_o) and the gage location (x_j, y_j) (Eq. (7)). This parameter allows one to model partial-area rain storm cases directly with one or more rainfall gages covering discrete areas of a watershed.

A related approach is implemented for spatial interpolation of radar data. Instead of the inverse distance, a restricted nearest neighbor approach is implemented. As a point interpolator, the Thiessen method is essentially a proximal or nearest distance neighbor technique (Salas et al., 2002). To interpolate radar data, the technique is to search over all radar grid locations and map the rainfall process value from the nearest distance location to the model grid cell center. First, (5) is used to obtain the distance d_{oi} from each radar pixel (x_j, y_j) to the grid cell location (x_o, y_o). We then determine the distance $d_{oi} = \min(d_{o1}, \ldots, d_{on})$, and subject it to the following restriction:

$$d_{oi} = \begin{cases} d_{o1} & d_{o1} \leqslant d_{max}, \\ 0 & \text{otherwise}. \end{cases} \qquad (8)$$

The weights in (4) are estimated for the case where $d_{oi} \leqslant d_{max}$ from:

$$w_j = \begin{cases} 1 & \text{for } j = i, \\ 0 & \text{for } j \neq i. \end{cases} \qquad (9)$$

This technique is used because the radar data are specified as an intensity or depth over a fixed area (typically a square grid cell). The radar cell geometry (size and orientation) can be different than the TREX model grid. A restricted nearest neighbor interpolator allows one to easily handle these geometric differences in a straightforward manner, and handle cases when the input radar grid does not cover the entire watershed, or when individual storm cells cover small areas.

A design storm method is implemented in order to effectively simulate Probable Maximum Precipitation (PMP) design storms. When estimating PMP for a particular watershed, the standard procedure is to determine an average rainfall depth for a specified duration over the entire watershed. A design storm is then estimated by distributing this depth in time using alternating blocks with the maximum at the 2/3 point, and in space using successive subtractions for subbasins (Cudworth, 1989). The PMP storm uses an index grid map of subbasins and a rainfall time series for each subbasin. A subbasin index grid map consists of integer values denoting the location of each subbasin ($i = 1, \ldots, nsubbasins$) in the watershed. A rainfall time series is entered for each subbasin i and the rainfall rate is applied uniformly over that subbasin (Fig. 1). In this way, we can mimic a spatially uniform interpolator that has been used for modeling extreme storms for Probable Maximum Floods in the western United States, termed the ''method of successive subtraction of subbasin PMP volumes'' (Cudworth, 1989, p. 59).

An extreme storm geometry is implemented to simulate extreme storms using depth—area—duration (DAD) data from an extreme storm catalog (USACE, 1945). The standard DAD information includes cumulative rainfall depths for specific durations and area sizes. Rain rates r [L/T] are determined by simple difference from each successive cumulative depth. The storm spatial distribution is a simple, parsimonious model based on DAD data. It is assumed that the storm is single-centered, and isohyets are geometrically similar in the form of an ellipse (Hansen et al., 1982; Wilson and Foufoula-Georgiou, 1990), where (x_s, y_s) is the storm center and a and b are major and minor axes, respectively (Fig. 2). This assumed storm shape describes both within-storm amounts and storm totals, and can be an adequate spatial representation based on the DAD data (Foufoula-Georgiou and Wilson, 1990). Although storm shapes are generally very complex, Hansen et al. (1982) recommended using a standardized elliptical pattern to represent the storm isohyets. The storm spatial pattern that is adopted has geometrically similar ellipses with a major (a) to minor (b) axis ratio c, where $c = a/b$ (Fig. 2). The storm orientation θ is defined clockwise in degrees from North (y) in the half-plane (0, 180), following Hansen et al. (1982). Using this geometry to represent a complete storm, the parameters are c and θ, and user-defined storm center (x_s, y_s). The ellipse parameter c is limited to [1.0, 8.0] where 1.0 represents a circle. Typical c values for extreme storms range between 1.0 and 3.0 (Hansen et al., 1982; Foufoula-Georgiou and Wilson, 1990). An example elliptical storm spatial distribution applied over the Arkansas River watershed (described below) is shown in Fig. 3.

Channel network

Several improvements are made to TREX to enable the modeling of channels on large watersheds, including: (1) modifications to topology/channel connectivity; (2) channel topology grid generation techniques; (3) channel bed smoothing; and (4) new spatial channel properties estima-
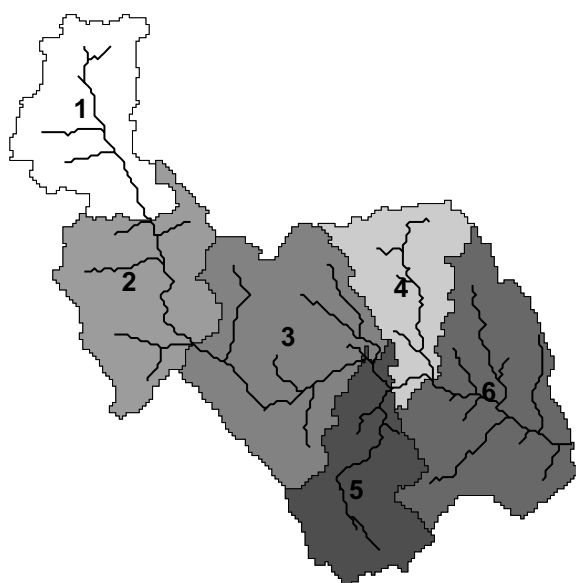

Figure 1 Spatially-uniform subareas (1 through 6) for PMP design storm application over Pueblo watershed.
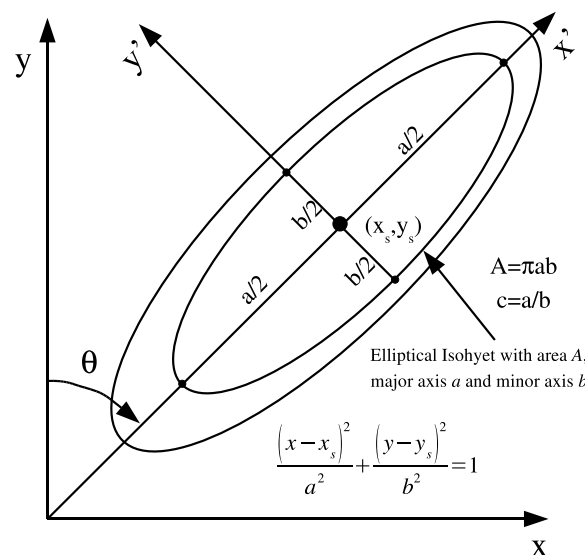

Figure 2 Storm spatial representation with storm center location (x_s, y_s), orientation θ, elliptical isohyets, and cartesian coordinate system.
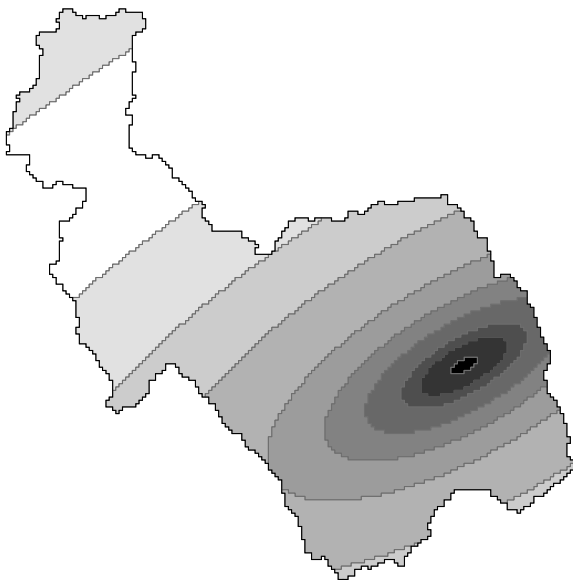
Figure 3 Example storm spatial distribution over the Arkansas River watershed with TREX. Rainfall is spatially uniform within each shaded ellipse area. The storm orientation angle is 60° (clockwise) from North.

Figure 4 Hypothetical channel connections between overland cells (squares) for a link with four nodes (numbered 1—4). Channel lengths are defined from grid cell center to grid cell center. Connections between nodes are either orthogonal or diagonal.

tion. Within the model, channels are segments that connect from overland grid cell center to grid cell center, and represent rivers or creeks in a watershed. The location of channel cells within the DEM is typically determined from stream network generation techniques within a GIS. The tool that is used to estimate the stream channel network and locations of channel cells as part of this research is TauDEM (Tarboton, 2005). Using this tool, we defined overland cells and channel cells using an area threshold.

The new topology feature that is required for modeling large watersheds is the ability for channel segments to be connected in eight directions, known as the D8 approach (Tarboton, 1997). The former CASC2D versions only supported channels connected in north—south or east—west directions on a side. The TREX topology routine is modified to directly use information from an 8D flow direction grid. This improves the channel length and slope representation in the model. A hypothetical channel connectivity case with four cells is shown in Fig. 4.

One difficult aspect of using TREX on large watersheds is the development of connectivity relationships required for modeling channels. In order to model channels, the user first specifies a stream network that defines the location of cells that contain channel segments (Fig. 4). The topology of this network is then used to specify two maps to TREX that contain the connectivity information. The first map is called a ''link'' map and contains a grid of integers that denote channel locations for each grid cell within the watershed, and how each channel segment or ''river reach'' is connected to another. Link segments now follow connectivity rules for flow modeling in eight directions (D8) from a grid (Tarboton, 2005). A ''node'' map is derived from a link map and contains integer numbers that designate the connectivity between each grid cell (and thus flow direction) within an individual link (river channel segment). For example, if a link contains four grid cells, these cells are num-
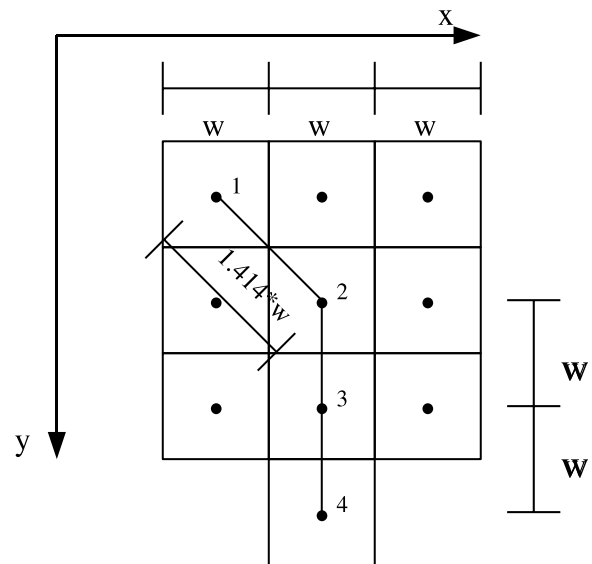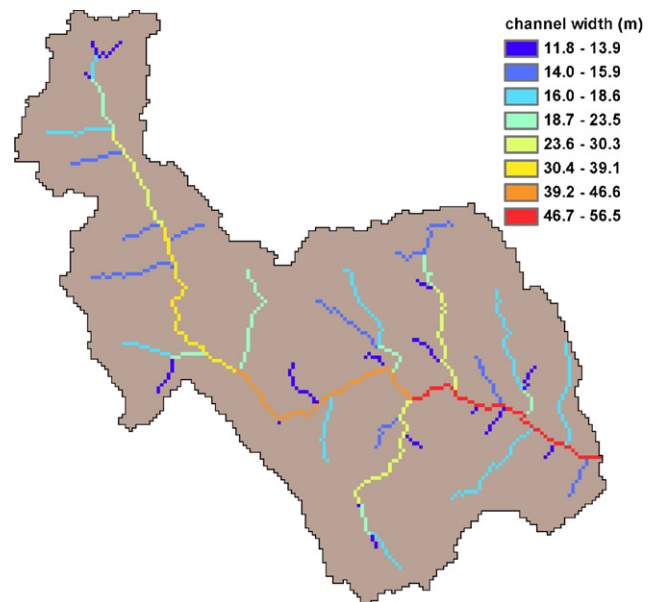

Figure 5 Example channel connectivity and spatially-varying channel widths in the Arkansas River watershed for TREX input. Grid cell size is 960 m; there are 69 links and 764 nodes.

bered 1, 2, 3 and 4 for that link (Fig. 4). New input preprocessing routines that automate development of channel (link/node) connectivity for TREX have been developed as part of this research. An example channel network map is shown in Fig. 5; many channel cells are connected on diagonals within the Arkansas River basin.

A new channel bed elevation checking and smoothing routine was developed to handle potentially flat slopes in channel cells. The basic problem considered here is zero

(flat) slopes in channel (stream network) cells within the watershed. The result is the model grid will not properly drain. This can be an important issue on large watersheds (>1000 km^2) when using ''larger'' (>150 m) grid cell sizes or due to problems with DEM quality in complex terrain. With larger grid cells, there can be many contiguous locations within the defined stream channel that have zero slopes. Several other researchers have noted the problems with flat slopes in DEMs and their effects on hydrologic modeling. Ogden et al. (1994) recognized adverse slopes and errors in channel slopes derived from DEMs. They proposed smoothing of the channel network using an ordered search and estimating the local slope from node to node, or by reducing the elevation of the cell by an arbitrary 25 cm amount using a 3-point moving average filter to smooth the final profile. Liu et al. (2003) recognized the problem with zero slopes along river corridors in the context of GIUH grid-based watershed modeling, and recommended modifying elevations to achieve some minimum slope in the floodplain and channel areas. In the context of TOPMODEL, Wolock and McCabe (1995) and Pan et al. (2004) recognized that zero slopes from DEMs cause problems calculating the $\ln(a/\tan \beta)$ index. They both provided simple solutions to flat areas. For areas with flat slopes, Wolock and McCabe (1995) redefined the local slope to be equal to (0.5 * vertical resolution)/(horizontal resolution). Pan et al. (2004) used Wolock and McCabe's assumption, and also tested an option where they flagged all cells in the watershed with flat slopes to be undefined, then reset slopes of all undefined cells to the minimum of all defined cell slopes. From this research, the solution to zero slope areas in TREX assumes a minimum slope between channel segments (nodes). The user enters this minimum slope value as a constant; it is then used to modify elevations of every node within a channel link where a zero slope is found between two nodes. The minimum slope estimate can be made using either (1) Wolock and McCabe's criterion or (2) some minimum value based on a DEM, channel slope estimates from topographic maps, vector data, or other source.

Another aspect of modeling channels in large watersheds with TREX is estimation of channel geometric properties, including base width, bank height, sideslope, dead storage depth, and channel sinuosity. These need to be estimated for each link and node in the channel network. The channel cross-section shape that TREX uses is a regular trapezoid, including rectangles or triangles as special cases. A semi-automated tool was developed to estimate channel properties, including spatially uniform, uniform within a link, and spatially varying properties from node to node options using downstream hydraulic geometry concepts. Widths w and depths d are estimated using power functions based on drainage area of the form $w = aA^b$ (Orlandini and Rosso, 1998) and $d = eA^f$ and field data from the watershed. Based on data collected at 20 sites in the Upper Arkansas River (England, 2006), estimated channel widths in the watershed are shown in Fig. 5.

Arkansas River application

The Arkansas River watershed in Colorado was selected to test the new TREX components and to demonstrate the model applicability for extreme storms and floods for practical applications. This research was conducted as part of a larger study to assess the overtopping risk of Pueblo Dam, a major water supply and flood control dam owned by the Bureau of Reclamation (England et al., 2006).

Watershed overview

The 11,900 km^2 Arkansas River study watershed is located just west of the city of Pueblo, Colorado (Fig. 6). Main tributaries include the East Fork Arkansas River, South Arkansas River, and Badger, Texas, Grape and Fourmile Creeks. The river cuts through the Colorado Front Range between about Cotopaxi and Cañon City. An important feature is the Royal Gorge, located just west of Cañon City. At the outlet of the Royal Gorge (Cañon City), the topography and river corridor change from steep canyons and narrow valleys to rolling terrain and an ever-widening river valley. The watershed falls within the Mountain and Plains flood hydrologic regions (Vaill, 2000). Snowmelt is the dominant runoff mechanism upstream of the Royal Gorge (England et al., 2006; Javier et al., 2007). Elevations in the watershed range from 4400 m (Mt. Elbert) to about 1430 m. Upstream of Cañon City, the mean elevation is 2911 m and the mean basin slope is 20.5%. Downstream of Cañon City, the basin is generally lower and flatter; the mean elevation is 1875 m and the mean slope is 9.9% within the watershed between Cañon City and Pueblo. We focus on flood runoff from this lower portion of the watershed downstream of the Royal Gorge and Cañon City, because the largest observed storms and floods center over this location (England, 2006).

Calibration and validation

In order to apply TREX to the Arkansas River above Pueblo, Colorado, GIS and field data were gathered to estimate model parameters. An elevation grid, obtained and processed from the USGS National Elevation Data set (NED), was used as the base for the watershed hydraulic routing. A 960 m grid cell size was used in the modeling to capture spatial variability and for fast model run times (Fig. 7a). The number of active grid cells in the 11,869 km^2 watershed is 12,879. Channels were derived using a 100 cell area threshold for initiation with 69 links and 764 channel cells. The model parameters to be estimated included Manning n for overland flow, and Green—Ampt parameters for effective porosity ϕ_e, effective suction head ψ, saturated hydraulic conductivity K_s and effective soil saturation S_e. Overland Manning n roughness values were estimated by correlation (Engman, 1986) with USGS National Land Cover Data set (NLCD) for nine land classes (Fig. 7b). Green—Ampt parameters were estimated based on the NRCS STATSGO soils database with 18 soils classes (Fig. 7c). Initial soil moisture S_e estimates were made based on rainfall and temperature station data (reported in climatological summaries and Monthly Weather Reviews), individual storm studies (USACE, 1945), and streamflow data.

A field reconnaissance was conducted within the basin on July 26—30, 2004 to locate paleoflood study sites and esti-
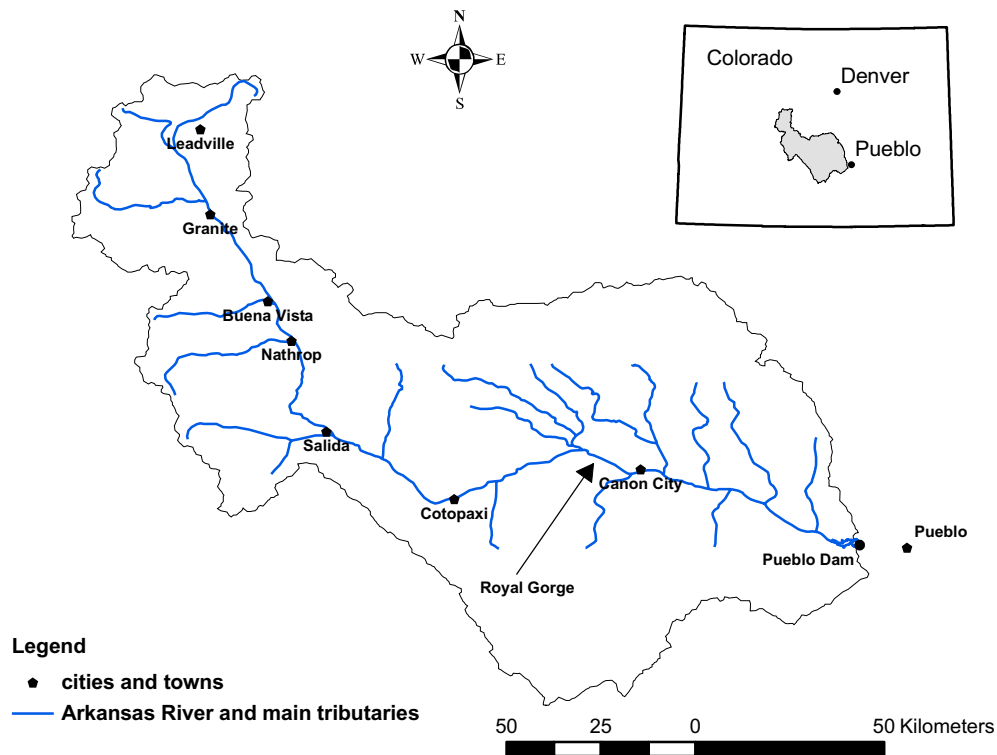
Figure 6 Arkansas River study watershed location map.

mate channel base width and bank height at 20 locations (England, 2006) using power functions. Widths ranged from 11 to 57 m (Fig. 5) with $a = 2.7$ and $b = 0.324$; bank heights ranged from 0.9 to 3.1 m with $e = 0.27$ and $f = 0.26$. A rectangular channel shape and sinuosity equal to 1.0 were assumed. Channel Manning n was assumed constant throughout the network, as detailed spatial roughness information was unavailable. This parameter influences the hydrograph timing and peak, and is subject to calibration as discussed below. The spatial distribution of channel widths and depths affects hydrograph runoff volumes and peaks. Channel widths and depths control the partitioning between overland and channel flows in TREX, and can dominate the in-channel hydraulic behavior as compared spatial differences in Manning n. Further data collection efforts are needed, as well as procedures for spatially-distributed Manning n estimates in watershed models.

Storm rainfall based on the DAD data (USACE, 1945; Hansen et al., 1988) for extreme storms was used as rainfall input. These data represent the most extreme storms in the Arkansas River basin for calibration and validation. Rainfall depths were specified in 6-h increments for various fixed area sizes, and the elliptical model was used to represent the spatial distribution of each storm. Constant time steps equal to 2.5 and 5 s, depending on rainfall inputs, were used to ensure computational stability for model simulations. The criteria used for calibration and validation were peak discharge, runoff volume, and time to peak of flood hydrographs. The parameters that were used to calibrate the model were Manning n for overland cells and channel segments, saturated hydraulic conductivity, and initial soil moisture.

The June 3—4, 1921 storm was selected for TREX model calibration. This flood was the largest on record in the Arkansas River basin near Pueblo, resulted in at least 78 deaths (Follansbee and Jones, 1922), and is one of the largest floods in Colorado. Rainfall amounts exceeded 30.5 cm in the storm core (Munn and Savage, 1922; Hansen et al., 1988). The peak flow was estimated to be about 2830 m^3/s (Follansbee and Jones, 1922), and has a return period of nearly 1000 years (England et al., accepted for publication). The calibration runoff data for this event were based on Munn and Savage (1922).

The results of the calibration are shown in Fig. 8. The model is stable, matches the peak discharge, flood volume and time to peak, and the hydrograph shape is close to the observed given the uncertainty in the data. Rainfall depth and water depth spatial results at the time of peak are shown in Fig. 9. Calibrated estimates of spatially varying Manning n (Fig. 7b) and saturated hydraulic conductivity K_s (Fig. 7c) are within published ranges (Engman, 1986; Rawls et al., 1993). Effective porosity and suction head parameters retained their initial values. The saturated hydraulic conductivity ranged from 0.13 to 28.5 cm/h, the effective porosity ranged from 0.35 to 0.47 cm^3/cm^3, and suction head ranged from 7.44 to 34.9 cm. A calibrated channel Manning n (0.050) was within the range of Colorado estimates (Jarrett, 1985). The initial soil moisture (effective saturation S_e) calibrated value for this event was 0.1, representative of the relatively dry pre-storm and flood conditions (Munn and Savage, 1922).

The model was validated with storm rainfall and runoff from the May 31, 1894 flood. This flood caused the third largest estimated peak flow on the Arkansas River at Pueblo
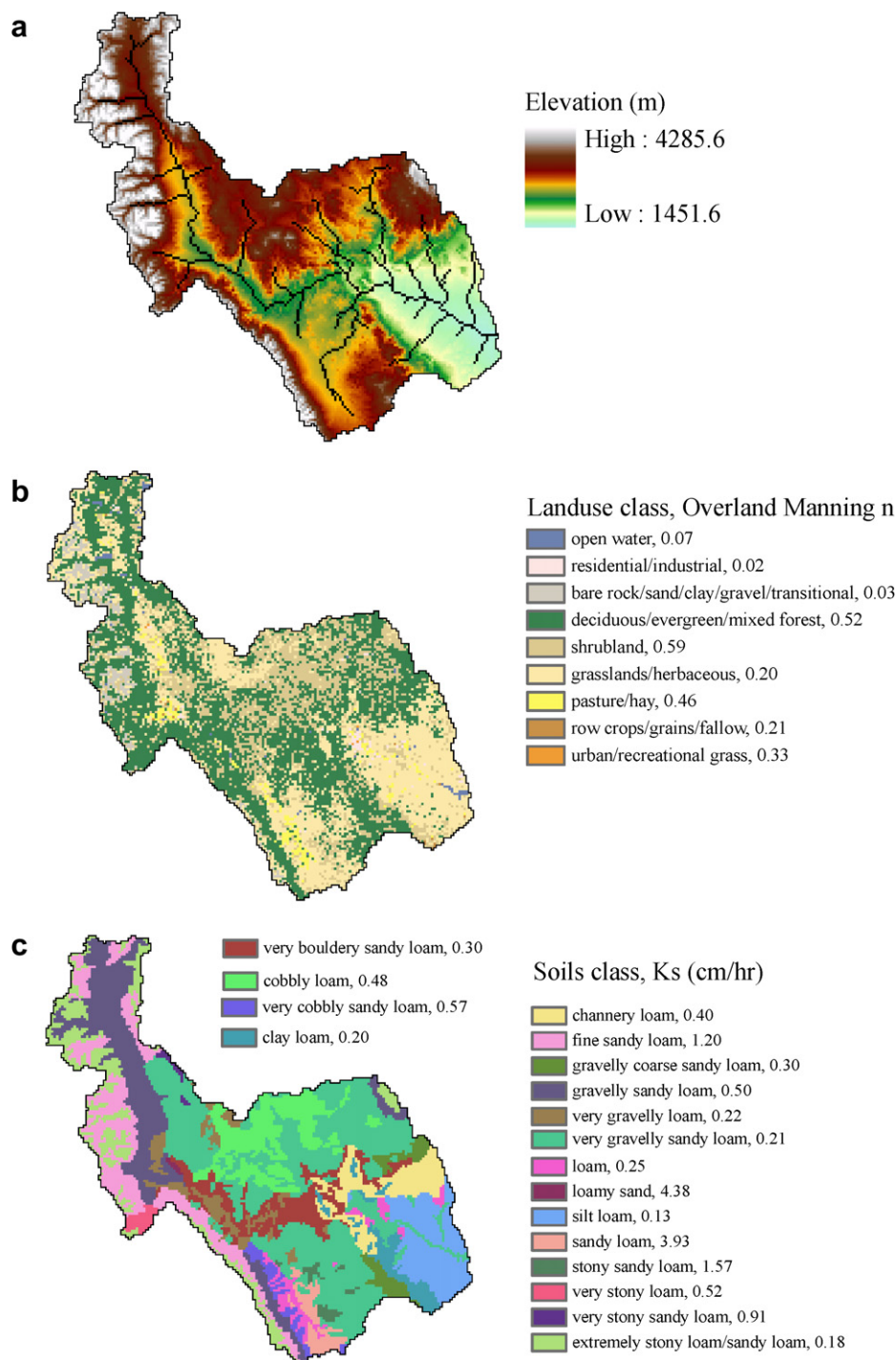
Figure 7 Arkansas River 960 m TREX GIS data layers: (a) elevation grid and channel cells; (b) land use classes and overland Manning n; (c) soils classes and saturated hydraulic conductivity K_s.

(England et al., accepted for publication), and was the most destructive flood in the history of the Arkansas valley prior to June 1921 (Follansbee and Jones, 1922). Space—time rainfall data for this event were obtained from Reclamation storm files and USACE (1945). This storm was of lower intensity and longer duration than June 1921; maximum point rainfall was 22.9 cm in 60 h. The flood flow for this event is based on USGS estimates at Cañon City and a peak flow estimate (1107 m³/s) at Pueblo.

The validation results are shown in Fig. 10. The initial soil moisture was increased to $S_e = 0.95$ so that the model matched the observed runoff data. This S_e value is close to the wet conditions observed prior to the extreme storm and flood (Munn and Savage, 1922). All other parameters retained their calibrated values. The spatial distributions of rainfall depth and water depth at the time of peak are shown in Fig. 11. The model matches the peak discharge, the approximate time to peak and the total flood runoff volume
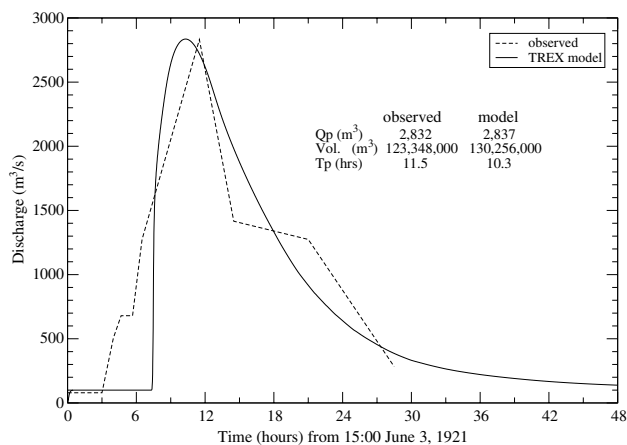
Figure 8 June 1921 extreme flood hydrograph and TREX model calibration.

within the uncertainty of the data. Given the storm rainfall, the validation run balances matching the peak flow at Pueblo and the runoff volume at Cañon. If the modeled peak flow at Pueblo were to increase, this would also increase the runoff volume at Cañon City. The other factor in the validation run is the potential errors in rainfall inputs. Fontaine (1995) shows that errors in precipitation data are the primary source of uncertainty in calibrating rainfall-runoff models for extreme floods. As the rainfall input data are inexact for this storm, changes in the rainfall forcing can have an effect on the validation. Initial soil moisture also has an effect on the runoff volume validation results for this storm.

Based on this calibration and validation, we suggest that the model can be used to simulate extreme floods on large watersheds on the order of 12,000 km^2 that are similar to the Arkansas River basin above Pueblo, Colorado. The model is stable and can reproduce the largest peaks and hydro-graphs that have been observed in this watershed. Ideally, we would have additional extreme flood data within this watershed for further TREX model testing. Unfortunately, for most large watersheds in the western United States with Bureau of Reclamation dams, including the Arkansas River, detailed extreme storm and flood data do not exist. The extreme flood data at Pueblo represent what is typically available in practice for most large watersheds ($\geqslant$1000 km^2) with dams. We are beginning to investigate model performance for extreme flood estimation on other western US watersheds as part of DMIP2 (Smith et al., 2006).

Runoff from probable maximum precipitation

The Bureau of Reclamation, like other Federal Agencies, relies on the Probable Maximum Precipitation (PMP) and the Probable Maximum Flood (PMF) as the upper limit for flood design. The use of PMP as input to TREX is explored to assess the overtopping potential for dam safety. We are unaware of any prior efforts to use a physically-based, distributed watershed model that has diffusive-wave routing similar to TREX to estimate runoff from PMP.

The storm rainfall input to TREX was the 72-h general storm PMP for Pueblo Dam (Bullard and Leverson, 1991) that was computed using HMR 55A (Hansen et al., 1988). Rainfall mass curves used a PMP standard temporal distribution with the maximum rainfall at the 2/3 point (48 h) of the storm (Cudworth, 1989), and were applied at six subareas (Fig. 1). The maximum rainfall total for subbasin 6 was 58.4 cm and the basin-average storm total rainfall was 34.8 cm.

The TREX model was run with the PMP mass curves and the calibrated TREX parameters, with S_e equal to 0.1. Two additional TREX runs were made to examine the effects of initial soil moisture with S_e = 0.5 and S_e = 0.8 that represent wetter conditions and watershed near saturation, respectively. The hydrograph results at Pueblo given PMP input
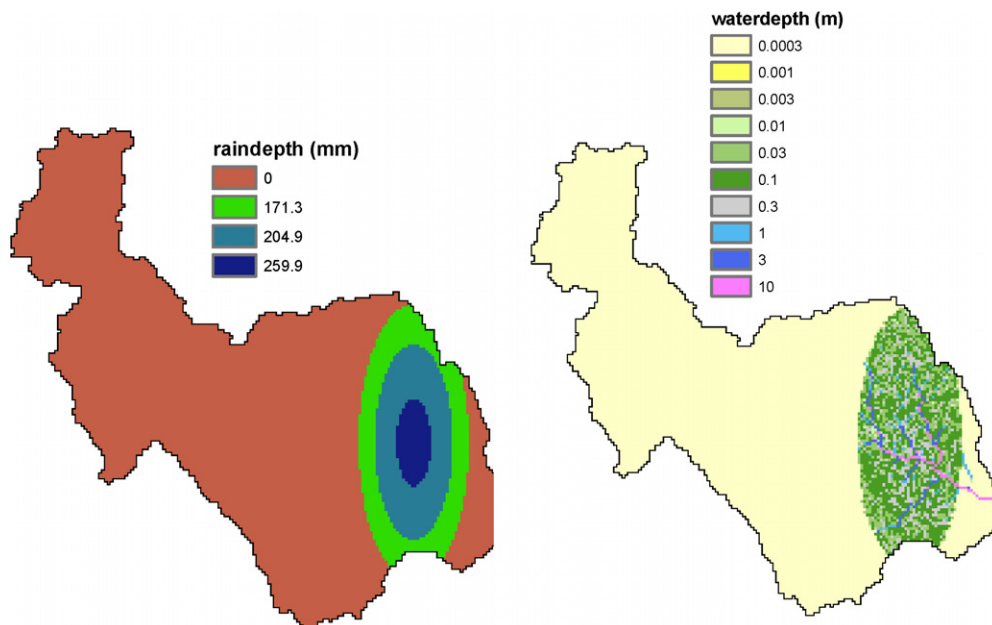

Figure 9 TREX June 1921 calibration cumulative rainfall and water surface depth at peak (10.3 h).
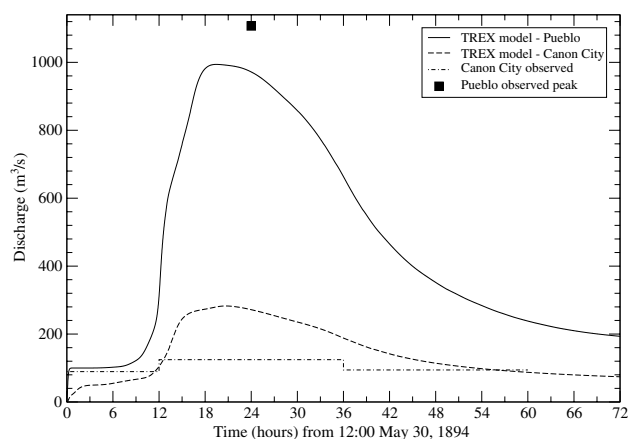
Figure 10 May 1894 extreme flood hydrographs and TREX model validation.

are shown in Fig. 12, and demonstrate that TREX can be used to estimate extreme floods up to and including those based on PMP. The PMP is the most extreme rainfall that is considered in hydrologic engineering for dam safety (Reclamation, 2002). The TREX runs based on PMP indicated that the model peak flows for this extreme rainstorm were relatively insensitive to initial soil moisture. Peaks increased 11% from $S_e = 0.1$ to $S_e = 0.8$. Initial soil moisture did have a somewhat larger effect on runoff volumes; the total hydrograph volume increased 27% from $S_e = 0.1$ to $S_e = 0.8$. Given PMP rainfall input, the TREX model with $S_e = 0.8$ has a very similar shape to the unit hydrograph-based PMF (Bullard and Leverson, 1991) (Fig. 12). The PMF peak flow is about 17% larger than the TREX prediction, and the PMF volume is about 67% larger. The much larger PMF volume is due to dramatically lower infiltration rates and use of a simple minimum, constant loss method (Cudworth, 1989) rather than Green—Ampt infiltration used in TREX (Velleux et al., 2006a).

Discussion

The Bureau of Reclamation is now utilizing hydrologic risk analysis to assess the safety of dams in the western United States. The deterministic PMF is still used by Reclamation as the maximum flood loading condition; if a dam can successfully pass the PMF, the (undefined) flood risk is assumed to be minimal. Reclamation is currently developing and applying tools and data sets to estimate extreme flood probabilities for dam safety (Swain et al., 2004). The work presented in this paper is one piece in our long-term, ongoing effort to improve understanding, estimation and prediction of extreme floods and probabilities, and have improved tools in place for use in dam safety practice. Here, we focused on estimating flood magnitudes up to the PMF using TREX; this is the initial application of the model for this purpose. However, hydrologic risk analysis also requires flood probability estimates. Rainfall-runoff models can be used to do this in a derived distribution framework (Bocchiola et al., 2003), via Monte-Carlo simulation (Nathan and Weinmann, 2004; USACE, 2005) and using probability-neutral concepts (Nathan and Weinmann, 1999). We are exploring the use of TREX for flood frequency with independent paleoflood data and flood frequency curves for model validation and will report on that work in the near future.

Recent work in extreme flood hydrometeorology (e.g. Giannoni et al., 2003; Hicks et al., 2005; Smith et al., 2005) has demonstrated the importance of watershed channel network, storm structure and evolution, terrain, land use effects and utility of radar data. Distributed models such as TREX can directly utilize these concepts in a computation-based, ''virtual experiment'' approach (e.g., Weiler and McDonnell, 2004). These models are one way to explore extreme flood questions and flood frequency curve extrapolations, especially beyond ''the credible limit of extrapolation'' (Nathan and Weinmann, 1999). One ongoing, major challenge is the availability of detailed, distributed data
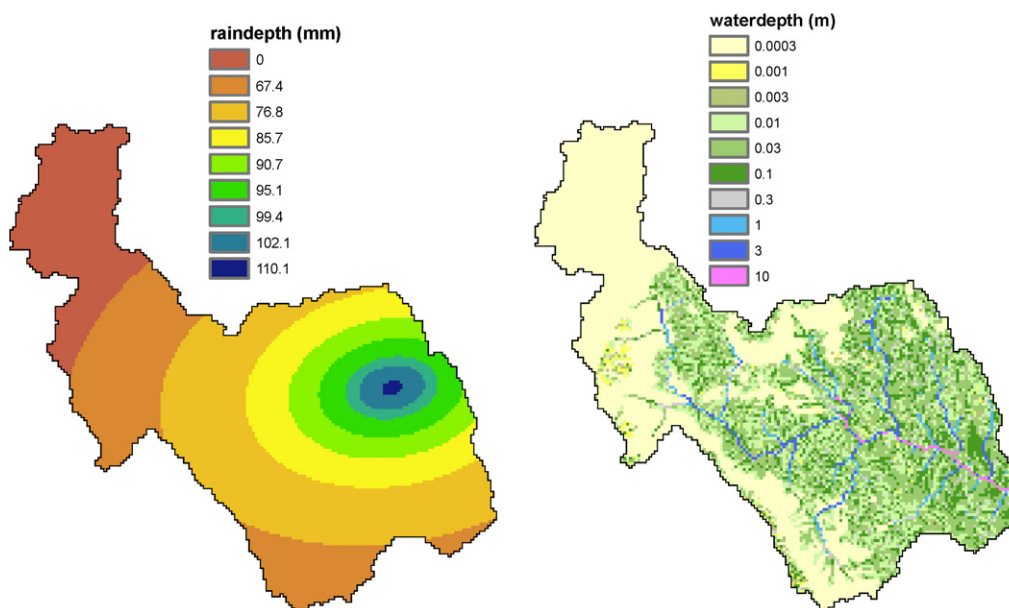

Figure 11 TREX May 1894 validation cumulative rainfall and water surface depth at peak (19.4 h).
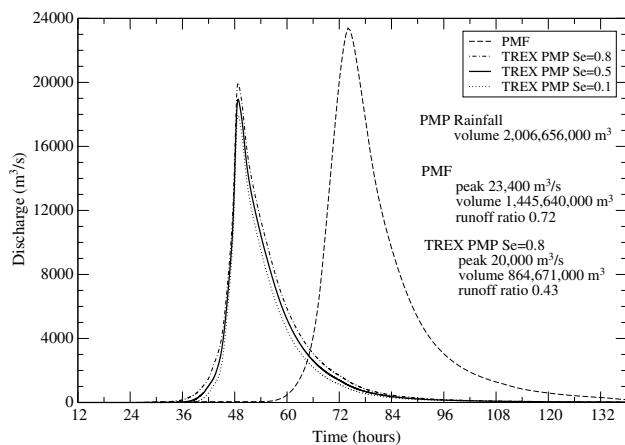
Figure 12 TREX PMP-based hydrographs with varying initial soil moisture and Reclamation PMF hydrograph.

sets relevant to extreme floods, such as radar rainfall, soil moisture, hydrographs at fine temporal scales, and soils information for parameter estimation and model testing. We are commencing additional model testing on other western US watersheds with more data.

Summary and conclusions

The focus of this research was to improve and test the Two-dimensional, Runoff, Erosion and Export (TREX) model (Velleux et al., 2006a) in order to simulate extreme flood processes on large watersheds in arid and semi-arid regions within the mountainous western United States. The objectives were to: (1) describe new extreme storm and channel process model components so that TREX could be applied to large watersheds and extreme floods; and (2) demonstrate these model features via calibration, validation and simulation of extreme storms and floods on a large (12,000 km^2) watershed, the Arkansas River at Pueblo, Colorado.

To enable extreme storm modeling on large watersheds, a spatial storm rainfall model was implemented within TREX and demonstrated on the Arkansas River basin. The storm model uses an elliptical pattern, depth-area duration data, and storm center, orientation and major-to-minor axis ratio parameters. A PMP design storm approach, that uses a sub-basin grid map and the method of successive subtractions, was also implemented and demonstrated. Other storm rainfall improvements included a linear interpolation technique for rainfall temporal observations, and restricted nearest-neighbor and inverse distance spatial interpolation techniques for radar and rain gages.

A channel topology algorithm was implemented that allows channels to be connected in eight directions. Automated tools for model link and node connectivity, channel bed smoothing, and channel geometry were described. The new channel mesh generator was developed to provide spatially-distributed channel geometry inputs to TREX. It was tested using power functions for bank heights and channel widths based on field data collected at 20 sites within the Arkansas River basin. TREX can be applied on large watersheds with an improved representation of channels and their connectivity in the watershed network.

The TREX model was applied to the 12,000 km^2 Arkansas River basin above Pueblo, Colorado. The model was calibrated to the June 1921 flood of record on the watershed. This flood had an approximate peak of 2830 m^3/s and a return period of about 1000 years. The calibrated peak discharge, volume and hydrograph shape were appropriate. The model was validated with the May 1894 flood, the third largest flood on record. Based on the calibration and validation, this model can simulate very extreme floods on large watersheds with limited data, as is typically found in dam safety practice.

The calibrated TREX model was then used to simulate the watershed response given a PMP design storm for Pueblo Dam. Results indicated that the model was stable and can be used to estimate an extreme flood based on the PMP. TREX results based on the PMP were generally comparable in terms of peak flow to a published PMF hydrograph at Pueblo, but runoff volumes were lower. Initial soil moisture changes had little effects on model peak flow predictions and hydrograph shape, but affected the total runoff volume.

Overall, it was shown that the TREX model can successfully be applied to a large watershed of this scale (12,000 km^2) and simulate extreme floods including that resulting from the Probable Maximum Precipitation. This physically-based, spatially-distributed model is an alternative to traditional lumped, unit-hydrograph models typically used to estimate Probable Maximum Floods.

References

Ambrose, R.B., Martin, J.L., Wool, T.A., 1993. WASP5, A Hydrodynamic and Water Quality Model — Model Theory, User's Manual, and Programmer's Guide. U.S. Environmental Protection Agency, Office of Research and Development, Environmental Research Laboratory, Athens, Georgia.

Australian Rainfall and Runoff (ARR), 2001. Volume One: A Guide to Flood Estimation (in eight books). The Institution of Engineers, Australia.

Beven, K.J., 1989. Changing ideas in hydrology — the case of physically-based models. J. Hydrol. 105, 157—172.

Beven, K.J., 2001. Rainfall-Runoff Modeling, The Primer. John Wiley and Sons, Chichester, 360 p.

Bocchiola, D., De Michele, C., Rosso, R., 2003. Review of recent advances in index flood estimation. Hydrol. Earth Sys. Sci. 7 (3), 283—296.

Bullard, K.L., Leverson, V., 1991. Pueblo Dam, Fryingpan-Arkansas Project Probable Maximum Flood (PMF) Study. Flood Section, Bureau of Reclamation, Denver, CO, Dated June, 1991, 23 p. and enclosures.

Bureau of Reclamation (Reclamation), 1990. Flood Hydrograph and Routing System (FHAR) Computer Model version 4.14, Technical Service Center, Denver, CO.

Bureau of Reclamation (Reclamation), 2002. Interim guidance for addressing the risk of extreme hydrologic events. Dam Safety Office and Technical Service Center, Denver, CO, 3 p.

Cecilio, C.B., Kraeger, B.A., Yucel, V., 1974. Spillway design for series of reservoirs. J. Hydraul. Eng., ASCE 100 (HY10), 1329–1342.

Cudworth Jr., A.G., 1989. Flood Hydrology Manual. A Water Resources Technical Publication, U.S. Department of Interior, Bureau of Reclamation, Denver, Colorado, 243 p.

D'Odorico, P., Rignon, R., 2003. Hillslope and channel contributions to the hydrologic response. Water Resour. Res., 39(5), 1113, pp. SWC 1-1–SWC 1-9.

Doe III, W.W., Saghafian, B., Julien, P.Y., 1996. Land-use impact on watershed response: the integration of two-dimensional hydrologic modelling and Geographic Information Systems. Hydrol. Process. 10, 1503–1511.

Dunne, T., 1998. Wolman Lecture: Hydrologic science ... in landscapes ... on a planet ... in the future. In: Hydrologic Sciences: Taking Stock and Looking Ahead, National Research Council, Washington, DC, pp. 10–43.

England Jr., J.F., 2006. Frequency analysis and two-dimensional simulations of extreme floods on a large watershed. Ph.D. Dissertation, Department of Civil Engineering, Colorado State Univ., Fort Collins, Colorado, 237 p.

England Jr., J.F., Klawon, J.E., Klinger, R.E., Bauer, T.R., 2006. Flood Hazard Study, Pueblo Dam, Colorado, Final Report, Bureau of Reclamation, Denver, CO, June, 160 p. ftp://ftp.usbr.gov/jengland/TREX/pueblo_floodhazard_finalreport.pdf.

England Jr., J.F., Klawon, J.E., Klinger, R.E., Bauer, T.R., Julien, P.Y., accepted for publication. Paleoflood hydrology and extreme flood frequency of the Upper Arkansas River, Colorado, USA. Geomorphology.

Engman, E.T., 1986. Roughness coefficients for routing surface runoff. J. Irrig. Drain. Eng., ASCE 112 (1), 39–53.

Follansbee, R., Jones, E.E., 1922. Arkansas River flood of June 3–5, 1921. U.S. Geological Survey Water-Supply Paper 487, 44 p.

Fontaine, T.A., 1995. Rainfall-runoff model accuracy for an extreme flood. J. Hydraul. Eng., ASCE 121 (4), 365–374.

Foufoula-Georgiou, E., Wilson, L.L., 1990. In search of regularities in extreme rainstorms. J. Geophys. Res. 95 (D3), 2061–2072.

Garbrecht, J., Shen, H.W., 1988. The physical framework of the dependence between channel flow hydrographs and drainage network morphometry. Hydrol. Process. 2, 337–355.

Giannoni, F., Smith, J.A., Zhang, Y., Roth, G., 2003. Hydrologic modeling of extreme floods using radar rainfall estimates. Adv. Water Resour. 26, 195–203.

Hansen, E.M., Schreiner, L.C., Miller, J.F., 1982. Application of Probable Maximum Precipitation Estimates — United States East of the 105th Meridian. Hydrometeorological Report No. 52, National Weather Service, Washington, DC, 168 p.

Hansen, E.M., Fenn, D.D., Schreiner, L.C., Stodt, R.W., Miller, J.F., 1988. Probable Maximum Precipitation Estimates — United States between the Continental Divide and the 103rd Meridian. Hydrometeorological Report No. 55A, National Weather Service, Silver Spring, MD, 242 p.

Hicks, N.S., Smith, J.A., Miller, A.J., Nelson, P.A., 2005. Catastrophic flooding from an orographic thunderstorm in the central Appalachians. Water. Resour. Res. 41, W12428, 17 p.

Hydrologic Engineering Center (HEC), 1998. HEC-1 Flood Hydrograph Package, User's Manual, CPD-1A, version 4.1. U.S. Army Corps of Engineers, Davis, CA, 434 p.

Hydrologic Engineering Center (HEC), 2006. Hydrologic Modeling System HEC-HMS, User's Manual, CPD-74A, version 3.0.1. U.S. Army Corps of Engineers, Davis, CA, 248 p.

Institute of Hydrology (IH), 1999. Flood Estimation Handbook (FEH) — Procedures for Flood Frequency Estimation (in five volumes). Institute of Hydrology, Wallingford, Oxfordshire, United Kingdom.

Jarrett, R.D., 1985. Determination of roughness coefficients for streams in Colorado. U.S. Geological Survey Water-Resources Investigations Report 85-4004, 54 p.

Javier, J.R., Smith, J.A., England, J., Baeck, M.L., Steiner, M., Ntelekos, A.A., 2007. The climatology of extreme rainfall and flooding from orographic thunderstorm systems in the upper Arkansas River Basin. Water Resour. Res., 43, W10410, doi:10.1029/2006WR005093, 13 p.

Johnson, B.E., Julien, P.Y., Molnar, D.K., Watson, C.C., 2000. The two-dimensional upland erosion model CASC2D-SED. J. Am. Water Resour. Assoc., AWRA 36 (1), 31–42.

Jorgeson, J.J., 1999. Peak flow analysis using a two-dimensional watershed model with radar precipitation data. Ph.D. Dissertation, Department of Civil Engineering, Colorado State Univ., Fort Collins, Colorado, 194 p.

Julien, P.Y., Rojas, R., 2002. Upland erosion modeling with CASC2D-SED. Int. J. Sed. Res. 17 (4), 265–274.

Julien, P.Y., Saghafian, B., 1991. CASC2D Users Manual — A Two Dimensional Watershed Rainfall-runoff Model. Civil Eng. Report CER90-91PYJ-BS-12, Colorado State University, Fort Collins, CO, 66 p.

Julien, P.Y., Saghafian, B., Ogden, F.L., 1995. Raster-Based hydrologic modeling of spatially-varied surface runoff. Water Resour. Bull., AWRA 31 (3), 523–536.

Laurenson, E.M., Mein, R.G., Nathan, R.J., 2006. RORB Version 5 Runoff Routing Model — User Manual, Department of Civil Engineering, Monash University; http://civil.eng.monash.edu.au/expertise/water/rorb.

Liu, Y.B., Gebremeskel, S., De Smedt, F., Hoffmann, L., Pfister, L., 2003. A diffusive transport approach for flow routing in GIS-based flood modeling. J. Hydrol. 283, 91–106.

Marco, J.B., Valdés, J.B., 1998. Partial area coverage distribution for flood frequency analysis in arid regions. Water Resour. Res. 34 (9), 2309–2317.

Marsik, M., Waylen, P., 2006. An application of the distributed model CASC2D to a tropical montane watershed. J. Hydrol. 330, 481–495.

Molnar, D.K., Julien, P.Y., 1998. Estimation of upland erosion using GIS. Comput. Geosci. 24 (2), 183–192.

Molnar, D.K., Julien, P.Y., 2000. Grid size effects on surface runoff modeling. J. Hydrol. Eng., ASCE 5 (1), 8–16.

Munn, J., Savage, J.L., 1922. The Flood of June 1921 in the Arkansas River, at Pueblo, Colorado. Trans. Am. Soc. Civ. Eng. 85, pp. 1–35, with discussion pp. 36–65.

Murphy, E.C. and others, 1906. Destructive Floods in the United States in 1905, with a discussion of flood frequency and an index to flood literature. U.S. Geological Survey Water-Supply Paper 162, 105 p.

Nathan, R.J., Weinmann, P.E., 1999. Estimation of Large to Extreme Floods: Book VI in Australian Rainfall and Runoff, A Guide to Flood Estimation. The Institution of Engineers, Australia.

Nathan, R.J., Weinmann, P.E., 2004. An improved framework for the characterization of extreme floods and for the assessment of dam safety. Hydrology: Science & Practice for the 21st Century, Vol. 1. Proc., British Hydrol. Soc., London, pp. 186–193.

Ogden, F.L., Julien, P.Y., 1993. Runoff sensitivity to temporal and spatial rainfall variability at runoff plane and small basin scales. Water Resour. Res. 29 (8), 2589–2597.

Ogden, F.L., Julien, P.Y., 2002. CASC2D: A two-dimensional, physically-based, Hortonian hydrologic model. In: Singh, V.P., Frevert, D. (Eds.), Mathematical Models of Small Watershed Hydrology and Applications. Water Resources Publications, Littleton, CO, pp. 69–112 (Chapter 4).

Ogden, F.L., Saghafian, B., Krajewski, W.F., 1994. GIS-Based channel extraction and smoothing algorithm for distributed hydrologic modeling. In: Cotroneo, G.V., Rumer, R.R. (Eds.), Proceedings, Hydraulic Engineering'94, American Society of Civil Engineers, Buffalo, NY, August 1—5, pp. 237—241.

Ogden, F.L., Sharif, H.O., Senarath, S.U.S., Smith, J.A., Baeck, M.L., Richardson, J.R., 2000. Hydrologic analysis of the Fort Collins, Colorado, flash flood of 1997. J. Hydrol. 228, 82—100.

Orlandini, S., Rosso, R., 1998. Parameterization of stream channel geometry in the distributed modeling of catchment dynamics. Water. Resour. Res. 34 (8), 1971—1985.

Paik, K., Kumar, P., 2004. Hydraulic geometry and the nonlinearity of the network instantaneous response. Water Resour. Res. 40, W03602, 7 p.

Pan, F., Peters-Lidard, C.D., Sale, M.J., King, A.W., 2004. A comparison of geographic information systems-based algorithms for computing the TOPMODEL topographic index. Water. Resour. Res. 40, W06303, 11 p.

Pilgrim, D.H., Cordery, I., 1993. Flood runoff. In: Maidment, D.R. (Ed.), Handbook of Hydrology. McGraw-Hill, New York, pp. 9.1—9.4 (Chapter 9).

Ponce, V.M., 1989. Engineering Hydrology, Principles and Practices. Prentice-Hall, NJ, 640 p.

Rawls, W.J., Ahuja, L.R., Brakensiek, D.L., Shirmohammadi, A., 1993. Infiltration and soil water movement. In: Maidment, D.R. (Ed.), Handbook of Hydrology. McGraw-Hill, New York, pp. 5.1—5.5 (Chapter 5).

Rojas-Sanchez, R., 2002. GIS-based upland erosion modeling, geovisualization and grid size effects on erosion simulations with CASC2D-SED. Ph.D. Dissertation, Department of Civil Engineering, Colorado State Univ., Fort Collins, Colorado, 140 p.

Saco, P.M., Kumar, P., 2002a. Kinematic dispersion in stream networks 1. Coupling hydraulic and network geometry. Water Resour. Res. 38(11), 1244, pp. 26-1—26-14.

Saco, P.M., Kumar, P., 2002b. Kinematic dispersion in stream networks 2. Scale issues and self-similar network organization. Water Resour. Res. 38(11), 1245, pp. 27-1—27-15.

Saco, P.M., Kumar, P., 2004. Kinematic dispersion effects on hillslopes. Water Resour. Res. 40, W01301, 12 p.

Saghafian, B., 1992. Hydrologic analysis of watershed response to spatially varied infiltration. Ph.D. Dissertation, Department of Civil Engineering, Colorado State Univ., Fort Collins, Colorado, 215 p.

Salas, J.D., Smith, R.A., Tabios, G.Q., Heo, J.-H., 2002. Statistical Computer Techniques in Water Resources and Environmental Engineering. Course notes, Department of Civil Engineering, Colorado State Univ., Fort Collins, Colorado.

Senarath, S.U.S., Ogden, F.L., Downer, C.W., Sharif, H.O., 2000. On the calibration and verification of two-dimensional, distributed, Hortonian, continuous watershed models. Water Resour. Res. 36 (6), 1495—1510.

Simanton, J.R., Osborn, H.B., 1980. Reciprocal-distance estimate of point rainfall. J. Hydraul. Eng., ASCE 106 (HY7), 1242—1246.

Singh, V.P., 1995. Computer Models of Watershed Hydrology. Water Resources Publications, Littleton, CO, 1130 p.

Smith, R.E., 2002. Infiltration theory for hydrologic applications. Water Resources Monograph 15, Am. Geophys. Union, Washington, DC, 212 p.

Smith, J.A., Sturdevant-Rees, P., Baeck, M.L., Larsen, M.C., 2005. Tropical cyclones and the flood hydrology of Puerto Rico. Water. Resour. Res. 41, W06020, 16 p.

Smith, M., Koren, V., Reed, S., Zhang, Z., Seo, D.-J., Moreda, F., Cui, Z., 2006. The Distributed Model Intercomparison Project: Phase 2 Science Plan. Hydrology Laboratory, Office Of Hydrologic Development, National Weather Service, 46 p.

Spah, J.A., 2000. Rainfall runoff and the effects of initial soil moisture associated with the Little Washita River Watershed, Oklahoma. M.S. Thesis, Department of Civil Engineering, Colorado State Univ., Fort Collins, Colorado, 140 p.

Swain, R.E., England Jr., J.F., Bullard, K.L., Raff, D.A., 2004. Hydrologic Hazard Curve Estimating Procedures. Dam Safety Research Report DS-04-08, Bureau of Reclamation, Denver, CO, 79 p.

Tabios, G.Q., Salas, J.D., 1985. A comparative analysis of techniques for spatial interpolation of precipitation. Water Resour. Bull., AWRA 21 (3), 365—380.

Tarboton, D.G., 1997. A new method for the determination of flow directions and upslope areas in grid digital elevation models. Water Resour. Res. 33 (2), 309—319.

Tarboton, D.G., 2005. TauDEM: Terrain Analysis Using Digital Elevation Models. Utah State University, Department of Civil and Environmental Engineering, http://hydrology.neng.usu.edu/taudem, May 2005.

Troch, P.A., Smith, J.A., Wood, E.F., de Troch, F.P., 1994. Hydrologic controls of large floods in a small basin: central Appalachian case study. J. Hydrol. 156, 285—309.

U.S. Army Corps of Engineers (USACE), 1945. Storm Rainfall in the United States (ongoing publication), Washington, DC.

U.S. Army Corps of Engineers (USACE), 2005. Stochastic modeling of extreme floods on the American River at Folsom Dam, flood frequency curve extension. Research Document RD-48, by MGS Engineering Consultants for Hydrologic Engineering Center, Davis, CA, 54 p.

Vaill, J.E., 2000. Analysis of the Magnitude and Frequency of Floods in Colorado. U.S. Geological Survey Water-Resources Investigations Report 99-4190, 35 p.

Velleux, M.L., England, J.F., Julien, P.Y., 2006a. TREX Watershed Modeling Framework User's Manual: Model Theory and Description. Department of Civil Engineering, Colorado State Univ., Fort Collins, August, 83 p.

Velleux, M., Julien, P.Y., Rojas-Sanchez, R., Clements, W.H., England, J., 2006b. Simulation of metals transport and toxicity at a mine-impacted watershed: California Gulch, Colorado. Environ. Sci. Technol. 40 (22), 6996—7004.

Velleux, M., Westenbroek, S., Ruppel, J., Settles, M., Endicott, D., 2001. A User's Guide to IPX, the In-Place Pollutant Export Water Quality Modeling Framework, Version 2.7.4. USEPA ORD, National Health and Environmental Effects Research Laboratory, Large Lakes Research Station, Grosse Ile, Michigan. 179 p. EPA/600/R-01/079.

Weiler, M., McDonnell, J., 2004. Virtual experiments: an new approach for improving process conceptualization in hillslope hydrology. J. Hydrol. 285, 3—18.

Wilson, L.L., Foufoula-Georgiou, E., 1990. Regional rainfall frequency analysis via stochastic storm transposition. J. Hydraul. Eng., ASCE 116 (7), 859—880.

Wolock, D.M., McCabe, G.J., 1995. Comparison of single and multiple flow direction algorithms for computing topographic parameters in TOPMODEL. Water. Resour. Res. 31 (5), 1315—1324.

Woolhiser, D.A., 1996. Search for physically based runoff model — a hydrologic El Dorado? J. Hydraul. Eng., ASCE 122 (3), 122—129.

Woolhiser, D.A., Smith, R.E., Giraldez, J.-V., 1996. Effects of spatial variability of saturated hydraulic conductivity on Hortonian overland flow. Water Resour. Res. 32 (3), 671—678.